Tradeoff Between Diversity Gain and Interference Suppression in a MIMO MC-CDMA System

Yan Zhang, *Student Member, IEEE*, Laurence B. Milstein, *Fellow, IEEE*, and Paul H. Siegel, *Fellow, IEEE*

***Abstract*—In this paper, the uplink of an asynchronous multi-carrier direct-sequence code-division multiple-access (MC-DS-CDMA) system with multiple antennas at both the transmitter and the receiver is considered. We analyze the system performance over a spatially correlated Rayleigh fading channel with multiple-access interference (MAI), and evaluate the antenna array performance with joint fading reduction and MAI suppression. Assuming perfect channel knowledge available at the transmitter, maximal ratio transmission is employed to weight the transmitted signal optimally in terms of combating signal fading. At the receiver, adaptive beamforming reception is adopted to both suppress MAI and combat the fading. Note that while correlations among the fades of the antennas in the receive array reduce the diversity gain against fading, the array still has the capability for interference suppression. We examine the effect of varying the number of transmit and receive antennas on both the diversity gain and the interference suppression.**

***Index Terms*—Beamforming, maximal ratio transmission (MRT), multi-carrier code-division multiple-access (MC-CDMA).**

I. Introduction

It HAS BEEN well understood that multiple antennas can increase the capacity and improve the performance of a wireless system. Both information and coding theoretic studies have shown significant diversity and coding gain for quasi-static wireless channels by employing multiple antennas at both the transmitter and the receiver. The main techniques already proposed to exploit those potential improvements at the transmitter side are: 1) space–time codes, which introduce redundancy across multiple antennas [1]; and 2) spatial multiplexing, which generates multiple independent symbol streams and transmits them through different antennas [2]. In these references, no channel state information (CSI) is required at the transmitter, and the power is assigned equally to each antenna.

Another antenna solution to improve the performance of wireless systems is adaptive beamforming when there is a dominant direction-of-arrival (DOA) for the signal of interest. For a transmit array, the channel information is used to focus as much energy in the direction of the receiver as possible. For a receive array, the gain of the antenna is maximized in the direction of the path with the strongest power. Compared with the spatial-diversity schemes mentioned above, beamforming is preferred in terms of complexity. On the other hand, beamforming, in general, has a much lower data rate compared with spatial multiplexing in a single-user multiple-antenna system. However, in a multiple-access channel, where K users, each with L_T transmit antennas, try to communicate with a common receiver with L_R receive antennas, beamforming is not only sufficient, but also necessary for achieving the so-called sum capacity of multiple-access channels, if the number of users is much larger than the number of receive antennas [3]. This latter condition generally holds in a code-division multiple-access (CDMA) system.

In this paper, an asynchronous multi-carrier direct-sequence (MC-DS) CDMA system with multiple antennas at both the transmitter and the receiver is considered. Assuming perfect channel knowledge available at the transmitter, maximal ratio transmission (MRT) is employed to weight the transmitted signal optimally in terms of combating signal fading. Adaptive beamforming reception is adopted to suppress multiple-access interference (MAI) and combat the fading. We analyze the system performance over a spatially correlated Rayleigh fading channel with MAI, and evaluate the antenna array performance with joint fading reduction and MAI suppression. The detailed organization of the paper is as follows. The system model and channel model used in the paper are described in Section II. Section III presents the analysis of system performance, and is followed by some numerical results and discussions in Section IV. Finally, conclusions are drawn in Section V.

II. System Model

A. Transmitter

We describe a system model exploiting multiple antennas in a single-cell MC-CDMA system. Assume that both the mobiles and the base station use an antenna array to transmit and receive signals, where each mobile has an antenna array of size L_T used for MRT [4], and the base station has an antenna array of size L_R used for adaptive beamforming reception. For the block diagram shown in Fig. 1, the transmitted signal vector of dimension $(L_T \times 1)$, in the mth subband for user k, is given by

$$\begin{aligned}\underline{s}_m^{(k)}(t) &= \sqrt{P_k}c_k(t)\underline{d}_m^{(k)} \exp\left[j\left(\omega_m t + \theta_m^{(k)}\right)\right] \\ &= \sqrt{P_k}\sum_{n=-\infty}^{\infty} c_n^{(k)} h(t-nT_c) u_{\lfloor n/N_s \rfloor}^{(k)} \\ &\quad \cdot \underline{v}_m^{(k)} \exp\left[j\left(\omega_m t + \theta_m^{(k)}\right)\right] \qquad (1)\end{aligned}$$

Paper approved by C. Tellambura, the Editor for Modulation and Signal Design of the IEEE Communications Society. Manuscript received April 14, 2003; revised September 30, 2004. This work was supported in part by the Center for Wireless Communications at University of California, San Diego (UCSD), in part by the Core Program of the State of California, and in part by the TRW Foundation. This paper was presented in part at the Milcom Conference, Boston, MA, October 2003.

Y. Zhang and L. B. Milstein are with the Department of Electrical and Computer Engineering, University of California, San Diego, La Jolla, CA 92093 USA (e-mail: yzhang@cts.ucsd.edu).

P. H. Siegel is with the Center for Magnetic Recording Research, University of California, San Diego, La Jolla, CA 92093 USA.

Digital Object Identifier 10.1109/TCOMM.2005.844963

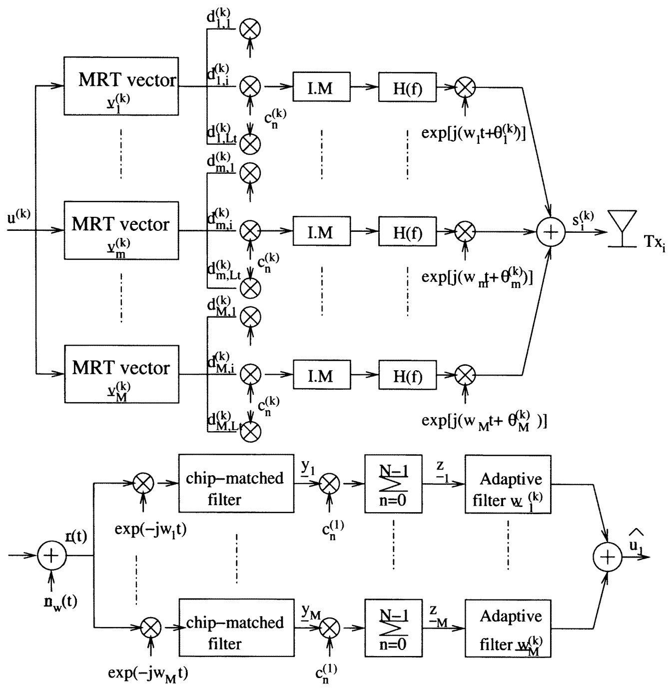

Fig. 1. Transceiver with adaptive beamforming in an MC-CDMA system.

where $u_i^{(k)}$ is the ith data symbol of user k, $\underline{v}_m^{(k)}$ is a transmission weight vector for user k in the mth subband, ω_m is the subcarrier frequency, $\theta_m^{(k)}$ is a random carrier phase associated with user k in the mth subcarrier band and is uniformly distributed over $[0, 2\pi)$, the spreading sequence of the interfering users $c_n^{(k)}$s, $k = 2, \ldots, K$, are assumed to be independent, identically distributed (i.i.d.) random variables taking values ± 1 with equal probability, while that of the desired user $c_n^{(1)}$ is taken to be deterministic, $h(t)$ is the impulse response of the baseband chip wave-shaping filter, and $1/T_c$ is the chip rate of a bandlimited MC-DS-CDMA system. We assume the chip wave-shaping filter $H(f)$ is bandlimited so that the spectra in each subband do not overlap. We also define $x(t) = F^{-1}|H(f)|^2$ and assume that $x(t)$ satisfies the Nyquist criterion, i.e., $x(nT_c) = \delta(n)$. The processing gain is defined as $N_s = T_s/T_c$, and is taken to be much smaller than the period of the spreading sequence, where T_s is the symbol duration. Then we can write the transmitted signal vector from the kth user as

$$\underline{s}^{(k)}(t) = \sqrt{P_k} \sum_{n=-\infty}^{\infty} u_{\lfloor n/N_s \rfloor}^{(k)} c_n^{(k)} h(t - nT_c) \cdot \sum_{m=1}^{M} \underline{v}_m^{(k)} \exp\left[j \left(\omega_m t + \theta_m^{(k)}\right)\right]. \quad (2)$$

B. Channel

The channel model is taken to be a slowly varying Rayleigh fading channel for each subcarrier, with transfer function $\xi_{m,r,l}^{(k)} = \alpha_{m,r,l}^{(k)} \exp(j\beta_{m,r,l}^{(k)})$, for $r = 1, \ldots, L_R$ and $l = 1, \ldots, L_T$, where l is the index for the transmit antennas and r is the index for the receive antennas. We assume that $\{\alpha_{m,r,l}^{(k)}\}$ and $\{\beta_{m,r,l}^{(k)}\}$ are statistically independent for different users, and that $\{\alpha_{m,r,l}^{(k)}\}$ and $\{\beta_{m,r,l}^{(k)}\}$ are, respectively, i.i.d. Rayleigh random variables with a unit second moment, and uniform random variables over $[0, 2\pi)$ for different transmit antennas. However, the array gain and the phase of the different elements in the receive antenna array are correlated, where the correlation is determined by parameters such as DOA $\phi_l^{(k)}$, angular spread $\Delta_l^{(k)}$, spacing between neighboring receive antennas D_r, and the wavelength of the carrier signal λ.

Specifically, using the model in [5], the composite channel gains for all the antennas in the array are represented as

$$\begin{aligned}\zeta_{m,i+1,l}^{(k)} &= \zeta_{m,1,l}^{(k)} \exp\left(-j2\pi i \sin \frac{\phi_l^{(k)}}{\lambda}\right) \\ &= \alpha_{m,l}^{(k)} \exp\left[j\left(\beta_{m,1,l}^{(k)}\right)' - j2\pi i \sin \frac{\phi_l^{(k)}}{\lambda}\right] \quad (3)\end{aligned}$$

where $(\beta_{m,r,l}^{(k)})' = \beta_{m,r,l}^{(k)} + \theta_m^{(k)}$ is uniformly distributed over $[0, 2\pi)$. If we make the additional, physically reasonable, assumption that the angles of arrival, $\phi_{l,n}^{(k)}$s, are uniformly distributed over $[\phi_l^{(k)} - \Delta_l^{(k)}, \phi_l^{(k)} + \Delta_l^{(k)}]$, a closed-form spatial correlation formula can be obtained [5]. That is

$$\begin{aligned}E\left[\zeta_{m,i,l}^{(k)} \left(\zeta_{m,j,l}^{(k)}\right)^*\right] &= Rs\left(\Delta_l^{(k)}, \phi_l^{(k)}, D_r, \lambda\right) \\ &= Rs_l^I(i,j) + jRs_l^Q(i,j) \quad (4)\end{aligned}$$

where $Rs_l^I(i,j)$ and $Rs_l^Q(i,j)$ are given by

$$\begin{aligned}Rs_l^I(i,j) &= J_0\left(\frac{2\pi D_r|i-j|}{\lambda}\right) + 2\sum_{n=1}^{\infty} J_{2n}\left(\frac{2\pi D_r|i-j|}{\lambda}\right) \\ &\quad \cdot \cos\left(2n\phi_l^{(k)}\right) \operatorname{sinc}\left(2n\Delta_l^{(k)}\right) \quad (5)\\ Rs_l^Q(i,j) &= 2\sum_{n=0}^{\infty} J_{2n+1}\left(\frac{2\pi D_r|i-j|}{\lambda}\right) \\ &\quad \cdot \sin\left((2n+1)\phi_l^{(k)}\right) \operatorname{sinc}\left((2n+1)\Delta_l^{(k)}\right) \quad (6)\end{aligned}$$

respectively, for $l = 1, \ldots, L_T$, and where the J_ns are Bessel functions of integer order. When this correlation is high, the signals at the antennas tend to fade at the same time, and the diversity benefit of antenna arrays against fading is significantly reduced. On the other hand, because independent fading is not required for interference suppression, antenna arrays can suppress interference, even with complete correlation. Thus, we need to evaluate the antenna array performance with joint fading reduction and interference suppression.

We define a channel matrix $H_m^{(k)}$ by putting the channel gain of each transmit and receive antenna pair in the mth subband into a matrix of size $L_R \times L_T$. That is to say, the i,jth entry in $H_m^{(k)}$ is $\xi_{m,i,j}^{(k)}$. Thus, the received signal vector in the antenna array is obtained as

$$\underline{r}(t) = \sum_{k=1}^{K} \sum_{m=1}^{M} H_m^{(k)} \underline{s}_m^{(k)}(t - \tau_k) + \underline{n}_w(t) \quad (7)$$

where τ_k is an arbitrary time delay uniformly distributed over $[0, T_s]$, and $\underline{n}_w(t)$ is the additive white Gaussian noise (AWGN) vector added to the receive antenna array, and each of its elements is a zero-mean complex Gaussian random process with two-sided spectral density η_0. An asynchronous MC-DS-CDMA is assumed, but the receiver is synchronized to the desired transmission, say that of user 1; thus, we assume that the power and delay of the desired signal are, respectively, $P_1 = 1$ and $\tau_1 = 0$, without loss of generality.

III. Performance Analysis

A. Output of the mth Correlator

We evaluate the performance of the first user. Perfect carrier, code, and bit synchronization are assumed. After down-converting to baseband, we can write the complex baseband received signal vector at the antenna array in the mth subband as

$$\begin{aligned}\underline{y}_m(t) &= \sum_{k=1}^{K}\sqrt{P_k}\sum_{n=-\infty}^{\infty}c_n^{(k)}h(t-nT_c-\tau_k)\\ &\quad\cdot u_{\lfloor n/N_s\rfloor}^{(k)}H_m^{(k)}\underline{v}_m^{(k)}\exp\left(j\theta_m^{(k)}\right)+\underline{n}_m(t)\\ &= \sum_{n=-\infty}^{\infty}u_{\lfloor n/N_s\rfloor}^{(1)}c_n^{(1)}h(t-nT_c)G_m^{(1)}\underline{v}_m^{(1)}\\ &\quad+\underline{i}_m^{(1)}(t)+\underline{n}_m(t)\end{aligned} \tag{8}$$

where

$$\underline{i}_m^{(1)}(t)=\sum_{k=2}^{K}\sqrt{P_k}\sum_{n=-\infty}^{\infty}u_{\lfloor n/N_s\rfloor}^{(k)}c_n^{(k)}h(t-nT_c-\tau_k)G_m^{(k)}\underline{v}_m^{(k)} \tag{9}$$

is the composite of MAI, and $(G_m^{(k)}) = H_m^{(k)}\exp(j\theta_m^{(k)})$ for $m = 1,\ldots,M$ and $k = 1,\ldots,K$. The noise is given by

$$\underline{n}_m(t)=\underline{n}_w(t)\exp(-jw_m t) \tag{10}$$

and is a complex AWGN process.

The output of the correlator during the ith symbol interval, obtained by summing the corresponding despread N_s chip-matched filter output samples in the mth branch, $\underline{z}_m^{(1)}(i)$, is given by

$$\begin{aligned}\underline{z}_m^{(1)}(i) &= \frac{1}{N_s}\sum_{n'=(i-1)N_s}^{iN_s-1}c_{n'}^{(1)}\left[\underline{y}_m(t)\star h(-t)\right]_{t=n'T_c}\\ &= \frac{1}{N_s}G_m^{(1)}\underline{v}_m^{(1)}\sum_{n'=(i-1)N_s}^{iN_s-1}c_{n'}^{(1)}\sum_{n=-\infty}^{\infty}c_n^{(1)}\\ &\quad\cdot u_{\lfloor n/N_s\rfloor}^{(1)}\int_{-\infty}^{\infty}h((n'-n)T_c+\tau)h(\tau)d\tau\\ &\quad+\underline{I}_m^{(1)}(i)+\underline{N}_m^{(1)}(i)\\ &= u_i^{(1)}G_m^{(1)}\underline{v}_m^{(1)}+\underline{I}_m^{(1)}(i)+\underline{N}_m^{(1)}(i)\end{aligned} \tag{11}$$

where $\star$ represents convolution. $u_i^{(1)}G_m^{(1)}\underline{v}_m^{(1)}$ is the signal component for the desired user

$$\underline{N}_m^{(1)}(i)=\frac{1}{N_s}\sum_{n=(i-1)N_s}^{iN_s-1}c_n^{(1)}\{\underline{n}_m(t)\star h(-t)\}_{|t=nT_c} \tag{12}$$

is the component due to thermal noise, and

$$\begin{aligned}\underline{I}_m^{(1)}(i) &= \sum_{k=2}^{K}\frac{\sqrt{P_k}}{N_s}\sum_{n'=(i-1)N_s}^{iN_s-1}c_{n'}^{(1)}\sum_{n=-\infty}^{\infty}u_{\lfloor n/N_s\rfloor}^{(k)}\\ &\quad\cdot c_n^{(k)}x\big((n'-n)T_c-\tau_k\big)G_m^{(k)}\underline{v}_m^{(k)}\\ &= \sum_{k=2}^{K}\frac{\sqrt{P_k}}{N_s}\sum_{n'=(i-1)N_s}^{iN_s-1}c_{n'}^{(1)}\\ &\quad\cdot\sum_{n=-\infty}^{\infty}\mu_n^{(k)}x\big((n'-n)T_c-\tau_k\big)G_m^{(k)}\underline{v}_m^{(k)}\\ &= \sum_{k=2}^{K}\frac{\sqrt{P_k}}{N_s}R_{k,1}(i)G_m^{(k)}\underline{v}_m^{(k)}\end{aligned} \tag{13}$$

is the MAI. In (13), $\mu_n^{(k)} = u_{\lfloor n/N_s\rfloor}^{(k)}c_n^{(k)}$ and

$$R_{k,1}(i)=\sum_{n'=(i-1)N_s}^{iN_s-1}c_{n'}^{(1)}\sum_{n=-\infty}^{\infty}\mu_n^{(k)}x\big((n'-n)T_c-\tau_k\big) \tag{14}$$

is the cross-correlation function of the spreading signal between user k and user 1 during the ith symbol interval. Here we absorb $u_{\lfloor n/N_s\rfloor}^{(k)}$ into $c_n^{(k)}$, since both are random variables taking values of ± 1 with equal probability. By the Lyapunov version of the central limit theorem, $\underline{I}_m^{(1)}(i)$ can be modeled as an asymptotically complex Gaussian vector as long as the following condition is satisfied [7]:

$$\sum_{n=-\infty}^{\infty}|x(nT_c-\tau)|<\infty$$

for all τ, where $0 \le \tau < T_c$.

B. Output of the Adaptive Beamformer

The correlator outputs from each receive antenna in each subband are combined with the beamforming vector $\underline{w}_1 = [(\underline{w}_1^{(1)})^T,\ldots(\underline{w}_M^{(1)})^T]^T$ to produce an estimate of the transmitted symbol of the desired user, where $\underline{w}_m^{(1)}$ is the beamforming vector for the mth subband, $m = 1,\ldots,M$. Define the correlator output vector $\underline{z}_1(i) = [(\underline{z}_1^{(1)}(i))^T,\cdots(\underline{z}_M^{(1)}(i))^T]^T$. Then the estimated data symbol can be represented as

$$\begin{aligned}\widehat{u}_{1,i} &= \underline{w}_1^{\dagger}\underline{z}_1(i)\\ &= S_{1,i}+I_{1,i}+N_{1,i}\end{aligned} \tag{15}$$

where † denotes complex conjugate

$$\begin{aligned} S_{1,i} &= \sum_{m=1}^{M} \left(\underline{w}_m^{(1)}\right)^{\dagger} \underline{S}_m^{(1)}(i) \\ &= u_i^{(1)} \sum_{m=1}^{M} \left(\underline{w}_m^{(1)}\right)^{\dagger} G_m^{(1)} \underline{v}_m^{(1)} \\ &= u_i^{(1)} \underline{w}_1^{\dagger} G_1 \underline{v}_1 \qquad (16) \\ I_{1,i} &= \sum_{m=1}^{M} \left(\underline{w}_m^{(1)}\right)^{\dagger} \underline{I}_m^{(1)}(i) \\ &= \sum_{k=2}^{K} \frac{\sqrt{P_k}}{N_s} R_{k,1}(i) \sum_{m=1}^{M} \left(\underline{w}_m^{(1)}\right)^{\dagger} G_m^{(k)} \underline{v}_m^{(k)} \\ &= \sum_{k=2}^{K} \frac{\sqrt{P_k}}{N_s} R_{k,1}(i) \underline{w}_1^{\dagger} G_k \underline{v}_k. \qquad (17) \end{aligned}$$

$G_k = \mathrm{diag}[G_1^{(k)} \dots G_M^{(k)}]$ for $k = 1, 2, \dots, K, \underline{v}_k = [(\underline{v}_1^{(k)})^T, \dots (\underline{v}_M^{(k)})^T]^T$, and

$$N_{1,i} = \sum_{m=1}^{M} \left(\underline{w}_m^{(1)}\right)^{\dagger} \underline{N}_m^{(1)}(i) \qquad (18)$$

$\underline{N}_1(i) = [(\underline{N}_1^{(1)}(i))^T, \dots (\underline{N}_M^{(1)}(i))^T]^T$.

Now we proceed to determine the optimum transmit and receive weight vectors $\underline{v}_1$ and $\underline{w}_1$, respectively, for the desired user. Since the MAI $\underline{I}_1(i)$ can be modeled as an asymptotically zero-mean complex Gaussian vector, and is independent of the AWGN vector $\underline{N}_1(i)$, the conditional signal-to-interference-plus-noise (SINR) γ_i of the estimated data $\widehat{u}_{1,i}$, conditioned on G_1, is given by

$$\begin{aligned} \gamma_i &= \frac{|S_{1,i}|^2}{\mathrm{Var}(I_{1,i}) + \mathrm{Var}(N_{1,i})} \\ &= \frac{\underline{w}_1^{\dagger} G_1 \underline{v}_1 \underline{v}_1^{\dagger} G_1^{\dagger} \underline{w}_1}{\underline{w}_1^{\dagger} E\left\{\frac{1}{2}\left[\underline{I}_1(i)\underline{I}_1^{\dagger}(i) + \underline{N}_1(i)\underline{N}_1^{\dagger}(i)\right]\right\} \underline{w}_1} \\ &\simeq \frac{|\underline{w}_1^{\dagger} G_1 \underline{v}_1|^2}{\underline{w}_1^{\dagger}\left[\sum_{k=2}^{K} \frac{P_k}{2N_s} R_I(0) \Gamma_k^{\dagger} R_{MI}^{(k)} \Gamma_k + \frac{\eta_0}{N_s} I_{ML_R}\right] \underline{w}_1} \qquad (19) \end{aligned}$$

where

$$\begin{aligned} \mathrm{Var}(I_{1,i}) &= \frac{1}{2} E\left[\underline{I}_1(i)\underline{I}_1^{\dagger}(i)\right] \\ &= \sum_{k=2}^{K} \frac{P_k}{2N_s}\left[R_I^{(k)}(0) + 2\sum_{m=1}^{N_s-1} R_I^{(k)}(mT_c) \cdot \sum_{n=m}^{N_s-1} c_n^{(1)} c_{n-m}^{(1)}\right] \Gamma_k^{\dagger} R_{MI}^{(k)} \Gamma_k \\ &\simeq \sum_{k=2}^{K} \frac{P_k}{2N_s} R_I(0) \Gamma_k^{\dagger} R_{MI}^{(k)} \Gamma_k. \end{aligned}$$

$R_I(\tau)$ is the autocorrelation of $R_{k,1}(i)$ [see (14)], Γ_k is a matrix given by

$$\Gamma_k = \begin{bmatrix} V_1^{(k)} & \cdots & 0 \\ \vdots & V_m^{(k)} & 0 \\ 0 & \cdots & V_M^{(k)} \end{bmatrix}$$

$$V_m^{(k)} = \underbrace{\begin{bmatrix} \underline{v}_m^{(k)} & \cdots & 0 \\ \vdots & \underline{v}_m^{(k)} & 0 \\ 0 & \cdots & \underline{v}_m^{(k)} \end{bmatrix}}_{L_R L_T \times L_R}$$

and $R_{MI}^{(k)}$ is a matrix whose elements are the crosscorrelations of the channel gains of user k. Refer to [7] for the detailed derivations of the covariance matrices for $\underline{N}_1(i)$ and $\underline{I}_1(i)$.

C. MRT and Adaptive Beamforming Reception

In statistically optimum beamforming, the weights are chosen based on the statistics of the data received at the array. Loosely speaking, the goal is to "optimize" the beamformer response, so the output contains minimal contributions due to noise and signals arriving from directions other than the desired signal direction. There are several different criteria for choosing statistically optimum beamformer weights, with perhaps the most obvious one being the maximization of the signal-to-noise ratio (SNR).

By using MRT, we set $\underline{v}_k = c_k G_k^{\dagger} \underline{w}_k$, where c_k is a constant used for normalization. Subject to the transmit power constraint $\|\underline{v}_k\|^2 = 1$, we have $|c_k| = (1/\|G_k^{\dagger}\underline{w}_k\|)$. Then the transmit weight vector is given by

$$\underline{v}_k = \frac{G_k^{\dagger}\underline{w}_k}{\left\|G_k^{\dagger}\underline{w}_k\right\|}. \qquad (20)$$

After using (20) in (19), and considering $k = 1$ as the desired user, we obtain

$$\begin{aligned} |S_{1,i}|^2 &= \left|\underline{w}_1^{\dagger} G_1 \underline{v}_1\right|^2 \\ &= \underline{w}_1^{\dagger} G_1 G_1^{\dagger} \underline{w}_1. \qquad (21) \end{aligned}$$

Now the goal is to choose beamforming weight vector $\underline{w}_1$ which maximizes the SNR γ_i of (19). Subject to the normalization constraint, we have

$$\widehat{\underline{w}}_1 = \arg\max_{\|\underline{w}_1\|^2=1} \frac{\underline{w}_1^{\dagger} G_1 G_1^{\dagger} \underline{w}_1}{\underline{w}_1^{\dagger} R_{IN}^{(1)} \underline{w}_1} \qquad (22)$$

where $R_{IN}^{(1)} = \sum_{j=2}^{K}((P_k)/(2N_s))R_I(0)\Gamma_j^{\dagger}R_{MI}^{(j)}\Gamma_j + ((\eta_0)/(N_s))I_{ML_R}$. Then the optimum weight vector $\widehat{\underline{w}}_1$ is the principal eigenvector of $(R_{IN}^{(1)})^{-1}G_1G_1^{\dagger}$, and γ_i is the corresponding eigenvalue [6], i.e., the maximum eigenvalue of $(R_{IN}^{(1)})^{-1}G_1G_1^{\dagger}$.

To compute $\widehat{\underline{w}}_1$, we need matrix Γ_k of user k, consisting of the transmit weight vector $\underline{v}_k$. However, this is not available, since it depends on receive weight vector $\underline{w}_k$ [see (22)], which, in turn, cannot be computed without the knowledge of $\underline{v}_j$ for $j \neq k$ [see (22)]. So we cannot apply (20) directly to get the optimum weight vector $\widehat{\underline{w}}_1$. As a consequence, one alternative is to use an iterative algorithm to solve the problem. Initially, we assume that $\underline{v}_k$ is an equal-weight vector, i.e., we weight each branch equally. Now it is possible to compute the beamforming weight vector $\hat{\underline{w}}_k$ for each user using (22). In turn, we can compute the corresponding transmit weight vector $\underline{v}_k$ for each user using (20). By using these updated $\underline{v}_k$s, we further update the $\hat{\underline{w}}_1$ iteratively until no improvement of SNR can be observed. This algorithm is quite complicated, in that the receiver has to recalculate the receive weight vector and feed it back to the corresponding transmitter. Note that this has to be done for all users any time there is a noticeable change of state for any one of them. As just one example, this is has to be done whenever the number of active users changes in the system.

Considering the complexity of adjusting the receive and transmit weight vectors based upon the corrresponding CSI for all the active users, and the computational complexity that this involves, as an alternative, we can replace the optimum criterion which maximizes SNR with an *ad hoc* criterion which only maximizes the received power for the desired user. Following the steps described above, we obtain the optimum receive weight vector $\underline{w}_m^{(1)}$ for each subband as

$$\hat{\underline{w}}_m^{(1)} = \arg \max_{\|\underline{w}_1\|^2=1} \left\{ \left| \left(\underline{w}_m^{(1)}\right)^\dagger G_m^{(1)} \left(G_m^{(1)}\right)^\dagger \underline{w}_m^{(1)} \right|^2 \right\}. \tag{23}$$

Therefore, the receive weight vector $\hat{\underline{w}}_m^{(1)}$ is the scaled principal eigenvector of $G_m^{(1)}(G_m^{(1)})^\dagger$, and the received power in each subband $P_{r,m}^{(1)}$ is the corresponding eigenvalue, i.e., the maximum eigenvalue $\hat{\lambda}_m$ of $G_m^{(1)}(G_m^{(1)})^\dagger$. Although it is difficult to find the probability density function (pdf) $p_{\hat{\lambda}_m}(\lambda)$ of $\hat{\lambda}_m$ for the ensemble of matrices $G_m^{(1)}(G_m^{(1)})^\dagger$, bounds on the $\hat{\lambda}_m$ can be easily found. The fact that $G_m^{(1)}(G_m^{(1)})^\dagger$ is a Hermitian and positive semi-definite matrix guarantees its eigenvalues to be nonnegative. Hence, the $\hat{\lambda}_m$ are bounded by

$$\begin{aligned} \frac{\sum_{l=1}^{L_R} \lambda_l}{L_R} &\le \frac{\sum_{l=1}^{L_R} \lambda_l}{\operatorname{rank}\left(G_m^{(1)}\left(G_m^{(1)}\right)^\dagger\right)} \\ &\le \hat{\lambda}_m \le \sum_{l=1}^{L_R} \lambda_l \\ &= \operatorname{Tr}\left(G_m^{(1)}\left(G_m^{(1)}\right)^\dagger\right) \end{aligned} \tag{24}$$

where $\operatorname{rank}(G_m^{(1)}(G_m^{(1)})^\dagger) \le \min(L_T, L_R)$, and $\operatorname{Tr}(\cdot)$ is the trace of the matrix. Therefore

$$\begin{aligned} \frac{\operatorname{Tr}\left(G_m^{(1)}\left(G_m^{(1)}\right)^\dagger\right)}{L_R} &\le P_{r,m}^{(1)} \\ &\le \operatorname{Tr}\left(G_m^{(1)}\left(G_m^{(1)}\right)^\dagger\right) \\ &= \sum_{l=1}^{L_T} \sum_{r=1}^{L_R} \left|\zeta_{m,r,l}^{(1)}\right|^2 \\ &= L_R \sum_{l=1}^{L_T} \left|\alpha_{m,l}^{(1)}\right|^2. \end{aligned}$$

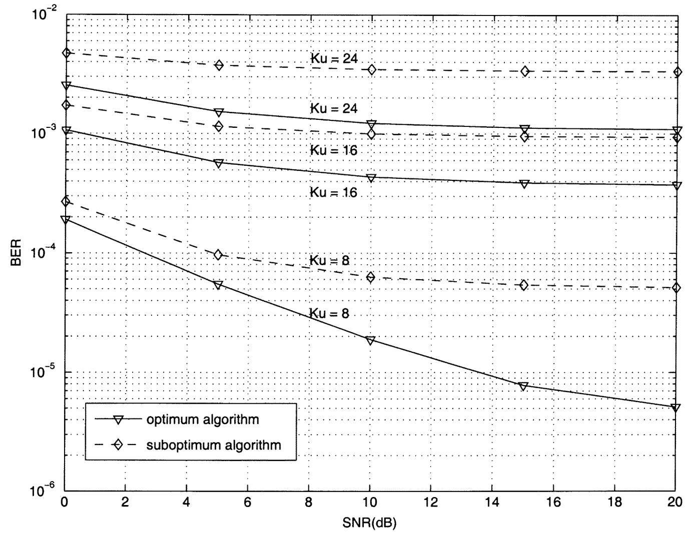

Fig. 2. Performance comparison of optimum algorithm and suboptimum algorithm for $M = 2$, $L_T = 2$, and $L_R = 4$ system with varying number of interfering users.

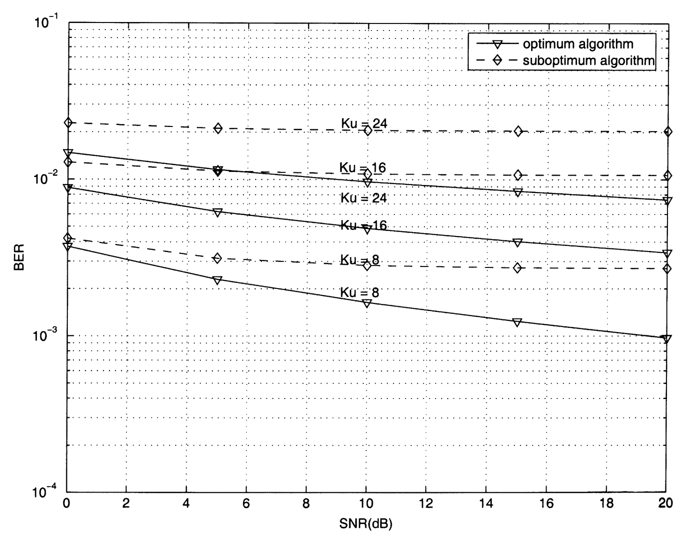

Fig. 3. Performance comparison of optimum algorithm and suboptimum algorithm for $M = 2$, $L_T = 1$, and $L_R = 8$ system with varying number of interfering users.

The last equality holds, since $\zeta_{m,r+1,l}^{(1)} = \alpha_{m,l}^{(1)} \exp(j(\beta_{m,1,l}^{(1)})' - j2\pi r \sin((\phi_l^{(1)})/(\lambda)))$ is assumed. Thus

$$P_r^{(1)} = \sum_{m=1}^{M} P_{r,m}^{(1)} \le L_R \sum_{m=1}^{M} \sum_{l=1}^{L_T} \left|\alpha_{m,l}^{(1)}\right|^2 \tag{25}$$

and we see that this scheme achieves a diversity of the order ML_T, since the $\alpha_{m,l}^{(1)}$s are assumed uncorrelated.

This scheme overcomes the disadvantages of the iterative algorithm, although it may suffer performance degradation. To quantify the performance loss, we resorted to simulation. We compared the performance of using the optimum algorithm and the suboptimum one, and the results are shown in Figs. 2–4. Note that in the low-SNR region, the additive noise is typically larger than the MAI (especially when the number of interfering users is small), and $R_{IN}^{(1)}$ is dominated by the covariance matrix

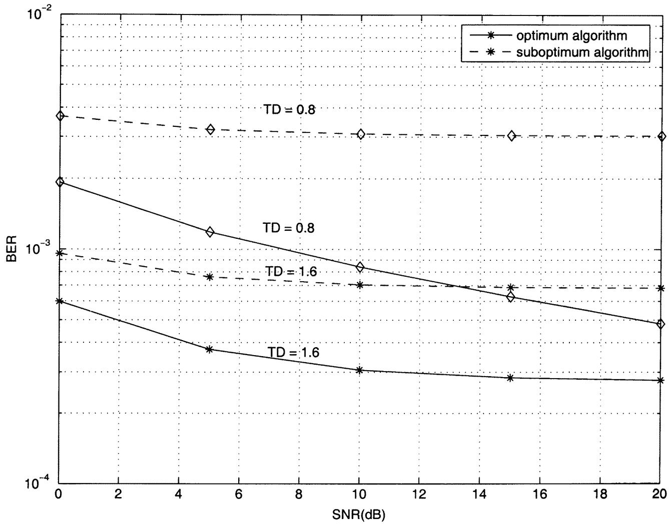

Fig. 4. Performance comparison of optimum algorithm and suboptimum algorithm for $M = 2$, $L_T = 2$, and $L_R = 4$ with different correlations among antennas.

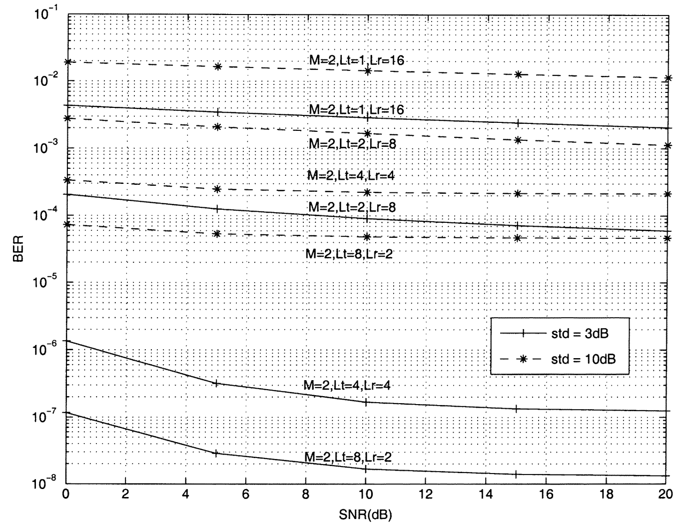

Fig. 5. BER versus E_b/η_0 for $K = 30$.

of the noise, which is a scaled identity matrix. Thus, optimizing the numerator term P_r is equivalent to optimizing the SNR γ_i. As expected, the results in these figures show that the gain achieved by using the iterative algorithm is not significant in the low-SNR region. As the SNR increases, the additive noise is no longer the dominant element. In the medium-to-high SNR region, the gain becomes more obvious by using the iterative algorithm. We further observe that the improvement is smaller when there are more interfering users in the system. It seems that when the number of interfering users is large, the covariance matrix of the MAI, $\sum_{k=2}^{K}((P_k)/(2N_s))R_I(0)\Gamma_k^{\dagger}R_{MI}^{(k)}\Gamma_k$, is close to a scaled identity matrix. Although we cannot give a rigorous mathematical proof, an intuitive explanation based on the numerical results is as follows. The elements along the main diagonal of each $R_{MI}^{(k)}$ are unity, while the off-diagonal elements are complex numbers whose norms are smaller than unity (this condition holds as long as the antennas in the array are not fully correlated, and the signals of different users arrive from directions uniformly distributed over $[-(\pi/2),(\pi/2)]$). Also, it can be shown that all the diagonal elements in the matrix $((P_k)/(2N_s))R_I(0)\Gamma_k^{\dagger}R_{MI}^{(k)}\Gamma_k$ are positive real numbers. The off-diagonal elements are still complex numbers, whose real and imaginary parts could be either positive or negative. So the more the terms are in the summation, the more likely the polarities of those off-diagonal elements are averaged out, and the more accurate is the approximation of the covariance matrix of the MAI, $\sum_{k=2}^{K}((P_k)/(2N_s))R_I(0)\Gamma_k^{\dagger}R_{MI}^{(k)}\Gamma_k$, looking like a scaled identity matrix. Thus, as the number of interfering users increases, the improvement by using the optimum criterion with the iterative algorithm diminishes.

When the correlations among the antennas in the receive array become smaller, so does the improvement from using the iterative algorithm, as observed in Fig. 4. As we know, when the antennas become less correlated, the off-diagonal elements in $R_{MI}^{(k)}$ are much smaller than unity, while the diagonal elements are unity. Thus, the approximation of $R_{MI}^{(k)}$ by an identity matrix is more appropriate, and there is less gain to be achieved by using the optimum algorithm.

IV. Numerical Results and Discussions

Given a fixed information rate and total bandwidth allocation, the product $MN_s = N^{sc}$ must be held constant, where N^{sc} is the processing gain of a single-carrier CDMA system and N_s is the corresponding value for each subcarrier in the MC-CDMA system. We assume that the fading seen by each of the transmit antennas is independent. At the receiver, L_R receive antennas are deployed for adaptive beamforming reception, where L_R can be a large enough number so that the fading experienced by each receive antenna might be correlated. M independent subcarriers can provide Mth-order frequency diversity gain, while L_T independent transmit antennas and L_R independent receive antennas result in an extra $L_T \cdot L_R$ order of spatial diversity gain. So fixing the value of $M \cdot L_T \cdot L_R$ fixes the maximal diversity gain achievable by the system. When the fading is, in fact, correlated, the diversity gain from the receive antenna array is reduced. However, independent fading is not required for interference suppression, so correlated receive antennas can still be used for MAI suppression. If we fix the product of $L_T \cdot L_R$, just for the sake of having a frame of reference for the performance tradeoff, then increasing L_T will increase the diversity gain against fading, while sacrificing the receive antenna array's capability of MAI suppression.

We assume the use of a raised-cosine filter characteristic, with rolloff factor $\alpha = 0.5$, for pulse shaping. We further assume the processing gain for a single-carrier system to be fixed at $N^{sc} = 32$. Since it is difficult to analytically derive the pdf of the instantaneous SNR, $f_\gamma(\gamma)$, we cannot obtain a closed-form expression for the bit-error rate (BER). To circumvent this problem, a Monte Carlo simulation is carried out. After one million trials, the SNR distribution of the combined outputs at the receiver is accumulated and $f_\gamma(\gamma)$ is numerically determined. The SNR value γ for each combined output is applied to the conditional bit-error probability for a binary phse-shift keying (BPSK) system, $\phi(\sqrt{2\gamma})$, and the average BER is calculated by integrating $Pe = \int_0^\infty \phi(\sqrt{2\gamma})f_\gamma(\gamma)d\gamma$.

In Fig. 5, we consider a MC-DS-CDMA system with 30 users, where the interference power is log-normally distributed with

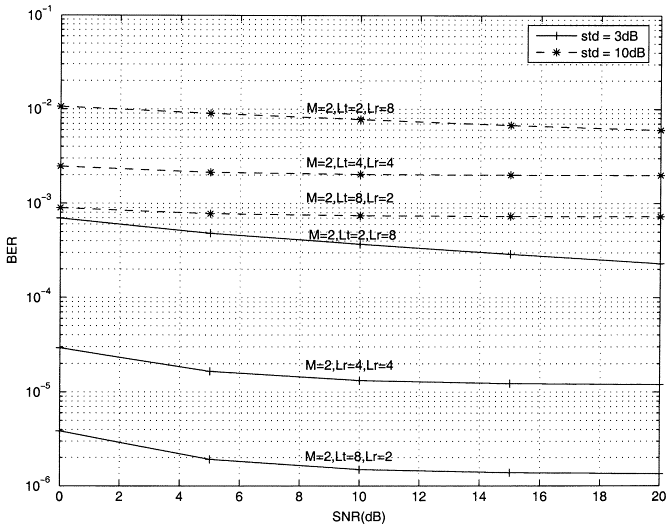

Fig. 6. BER versus E_b/η_0 for $K = 50$.

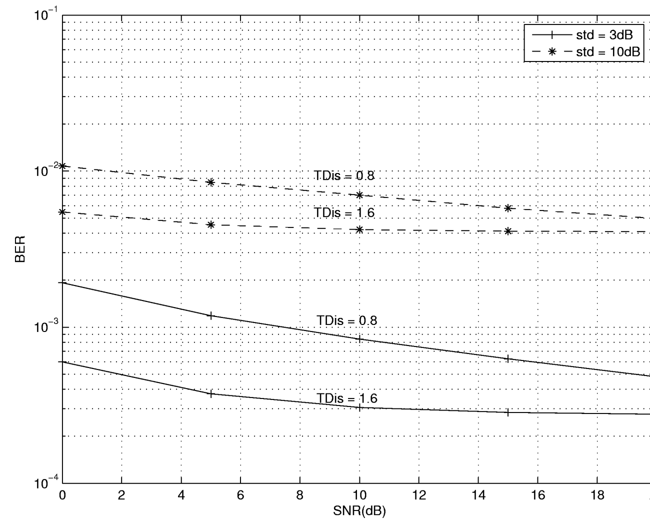

Fig. 7. BER versus E_b/η_0 for $K = 30$ and $L_T = 2, L_R = 4$ with varying correlations between receive antennas.

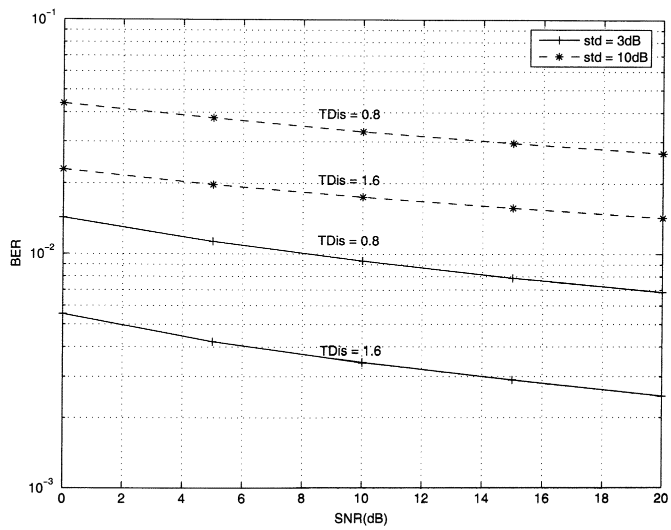

Fig. 8. BER versus E_b/η_0 for $K = 30$ and $L_T = 1, L_R = 8$ with varying correlations between receive antennas.

either a 3- or 10-dB standard deviation. The average BER versus E_b/η_0, for different sets of parameters, is shown in the figure. With the frequency diversity order fixed at $M = 2$, and $L_T \cdot L_R$ fixed at 16, we find that the system employing eight transmit antennas and two receive antennas is much better than one employing four transmit antennas and four receive antennas. This is primarily due to the eight-fold diversity gain from the eight transmit antennas with independent fading. Note that since the total length of the receive array is fixed at a value such that the multiple receive antennas experience correlated fading, the resulting effective diversity order achieved by the four-antenna array is less than twice that achieved by the two-antenna array, although the MAI suppression capability is enhanced with more receive antennas. We also compare in Fig. 5 the performance of other systems with the value of $M \cdot L_T \cdot L_R$ held constant. The worst case is $M = 2$, $L_T = 1$, and $L_R = 16$, since there is no transmit diversity gain, and most of the receive diversity-gain is lost due to the high correlations among the antennas in the receive array. We further evaluate the system performance with a more severe near–far problem, i.e., interference power is log-normally distributed with a 10 dB standard deviation. Compared with the system with better power control, the BER performance of all of the above systems degrades by at least one order of magnitude. It is further observed that the degradations are more significant for the systems with $L_R = 2$ receive antennas than they are for the systems with more receive antennas. This phenomenon can be explained as follows. The system's ability to suppress MAI is augmented by using more receive antennas, while sacrificing some diversity gain. Since MAI becomes more dominant in a system with a severe near–far problem, we find that the performance gap between the $L_R = 2$ and the $L_R = 4$, $L_R = 8$ or $L_R = 16$ systems decreases dramatically.

In Fig. 6, we plot BER performance curves for some of the systems in Fig. 5 when K is increased to 50. Compared with the curves plotted in Fig. 5 for systems with $K = 30$, there is smaller degradation when $L_R = 16$ receive antennas are employed. However, the degradation is much more conspicuous when $L_R = 2$, rather than $L_R = 16$, receive antennas are used. These observations indicate that systems with a larger number of receive antennas are more robust to various changes in the wireless environment, say, when the number of active users is constantly varying and/or the power control cannot be accurately implemented. Thus, it is beneficial to deploy more receive antennas in a dynamic wireless system to keep relatively stable service quality.

In Figs. 7 and 8, the BER performance, when the correlations among receive antennas are varied by changing the spacing between neighboring antennas, is shown. The fades become more correlated as we narrow the spacing. As we know, correlation results in loss of diversity gain against fading. However, the beamforming gain for MAI suppression is enhanced. This fact can be seen from the curves plotted in those two figures. When MAI is dominant, e.g., interference power distributed with 10 dB standard deviation, the performance degradation is much less than that in a system with better power control,

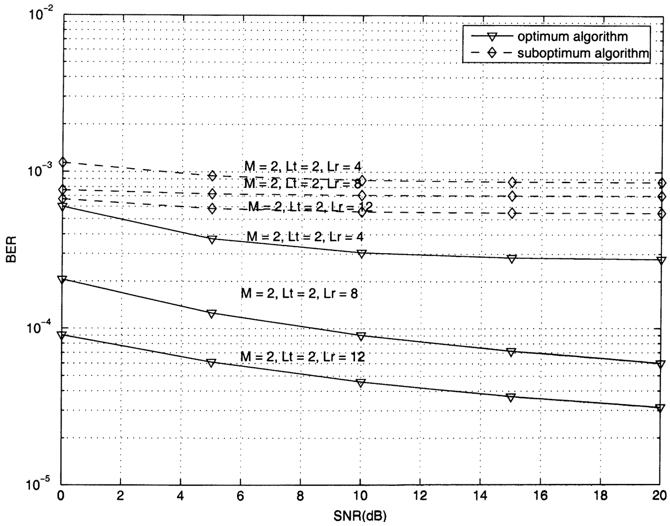

Fig. 9. BER versus E_b/η_0 for $K = 30$ and $N_s = 32$ per subcarrier with varying number of receive antennas.

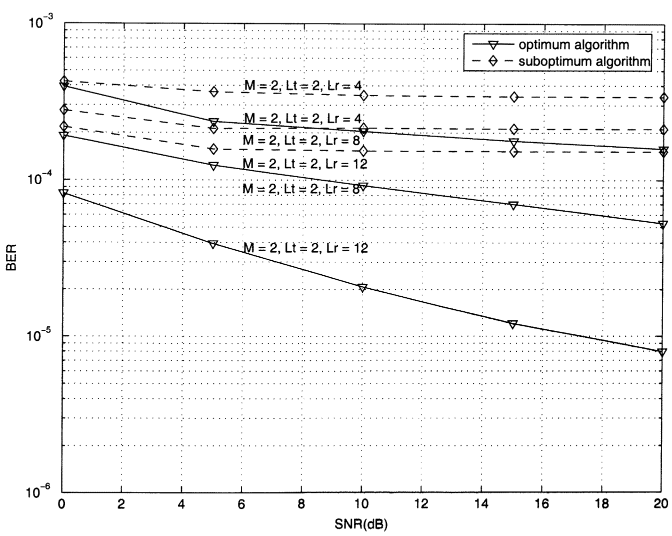

Fig. 10. BER versus E_b/η_0 for $K = 50$ and $N_s = 32$ per subcarrier with varying number of receive antennas.

where fading is the more dominant source of degradation. It is seen from the figures that the relative performance gap of the system with $L_T = 1,\ L_R = 8$ is larger than that of the system with $L_T = 2,\ L_R = 4$ when the correlations among the array increase due to a decrease in the spacing of neighboring antennas.

Note that while most of our results correspond to the product of $M \cdot L_T \cdot L_R$ being held constant, in Figs. 9 and 10, we show the effect of doubling and tripling the number of receive antennas while keeping both M and L_T constant, for both the optimum and the suboptimum algorithms. The resulting performance improvement is not as significant as might be expected. The reason is that we cannot double or triple the order of the diversity by doubling or tripling the number of receive antennas, since once again fades on the antennas become more correlated due to the decreasing distance between antenna elements. It is obvious from Figs. 9 and 10 that the performance improvement using the optimum algorithm is more significant than using the suboptimum algorithm when the number of receive antennas is increased. However, this performance gain is obtained at the expense of additional complexity, especially when the number of receive antennas is large. Furthermore, the performance gap between the optimum algorithm and the suboptimum algorithm will decrease if we consider using noisy channel estimates instead of the perfect CSI. This is because the optimum algorithm needs the CSI of all the users to calculate the weight vector for each user, whereas each receiver using the suboptimum algorithm only needs its own channel-state estimate. Last, from the Appendix, it is obvious that the number of calculations involved in the optimum algorithm is greater than that involved in the suboptimum algorithm.

V. Conclusion

In this paper, we proposed an MC-DS-CDMA system employing multiple antennas at both the mobile and the base station. MRT and adaptive beamforming reception are used to achieve the maximum received SINR for the desired user in a multiple-access channel with correlated Rayleigh fading. The conditional SNR is analytically derived, and the average BER is investigated via simulation. By varying the number of transmit antennas and receive antennas, we find a tradeoff between obtaining diversity gain against fading and MAI supression. In a spatially correlated Rayleigh fading channel, as long as the interferers arrive from directions uniformly distributed over $[-(\pi/2), (\pi/2)]$, using more receive antennas is preferred in a dynamic wireless system, since the effect of wireless environment changes (e.g., when the number of active users is varying and/or the accuracy of power control is varying) on the performance is smaller with more rather than less receive antennas. The benefit of using only a single transmit antenna is easier implementation in a small mobile unit. However, when the number of active users is stable and/or accurate power control is always maintained, using two independent transmit antennas with a smaller number of receive antennas is preferred.

Appendix

The complexity analysis for the two algorithms is shown as follows.

1) The computation complexity of the suboptimum algorithm:
   a) the number of multiplications

$$K\left[ML_R^2 L_T + M^2 L_R L_T\right]$$

   b) the number of divisions $K[ML_R + ML_T]$
   c) the number of other operations: KM eigenvalue decomposition of a square matrix of size L_R.
2) The computation complexity of the optimum algorithm depends on the number of iterations for convergence. In each iteration
   a) the number of multiplications

$$K\left[M^3 L_R^3 L_T + M^3 L_R^3 L_T^2 + 2M^3 L_R^2 L_T + M^2 L_R L_T\right]$$

b) the number of divisions $K[ML_R + ML_T]$
c) the number of other operations: K eigenvalue decomposition and inversion of a square matrix of ML_R.

Outside the loop, the number of multiplications is $M^3 L_R^2 L_T$.

According to the simulation results, empirically, the number of iterations ranges from 3 to 11, which depends on the specific value for each parameter, K, M, L_T, and L_R. Generally, the number of iterations increases as K or L_R increases.

REFERENCES

[1] V. Tarokh, N. Seshadri, and A. R. Calderbank, "Space–time codes for high data rate wireless communication: Performance criterion and code construction," *IEEE Trans. Inf. Theory*, vol. 44, no. 2, pp. 744–765, Mar. 1998.

[2] G. J. Foschini, "Layered space–time architecture for wireless communication in a fading environment when using multiple antennas," *Bell Labs Tech. J.*, vol. 1, pp. 41–59, Autumn 1996.

[3] W. Rhee and J. M. Cioffi, "On the asymptotic optimality of beamforming in multi-antenna Gaussian multiple access channels," in *Proc. Globecom*, vol. 2, San Antonio, TX, Nov. 2001, pp. 891–895.

[4] T. K. Y. Lo, "Maximum ratio transmission," *IEEE Trans. Commun.*, vol. 47, no. 10, pp. 1458–1461, Oct. 1999.

[5] J. Salz and J. H. Winters, "Effect of fading correlation on adaptive arrays in digital wireless communications," in *Proc. IEEE Int. Conf. Commun.*, Nov. 1993, pp. 1768–1774.

[6] B. D. Van Veen and K. M. Buckley, "Beamforming: A versatile approach to spatial filtering," *IEEE Acoust., Speech, Signal Process. Mag.*, pp. 4–24, Apr. 1988.

[7] Y. Zhang, "Performance of combined beamforming and space-time coding in a CDMA system," Ph.D. dissertation, Univ. Calif. San Diego, La Jolla, CA.

[8] B. Lu and X. Wang, "Iterative receivers for multiuser space–time coding systems," *IEEE J. Sel. Areas Commun.*, vol. 18, no. 11, pp. 2322–2335, Nov. 2000.

Yan Zhang (S'03) received the B.E. and M.E. degrees in radio engineering from Southeast University, Nanjing, China, in 1996 and 1999, respectively. Since 1999, she has been working toward the Ph.D. degree at the University of California, San Diego.

Her research interests include physical-layer communication theory, multiple-antenna techniques, information theory, spread spectrum, and channel coding.

Laurence B. Milstein (S'66–M'68–SM'77–F'85) received the B.E.E. degree from the City College of New York, New York, NY, in 1964, and the M.S. and Ph.D. degrees in electrical engineering from the Polytechnic Institute of Brooklyn, Brooklyn, NY, in 1966 and 1968, respectively.

From 1968 to 1974, he was with the Space and Communications Group of Hughes Aircraft Company, and from 1974 to 1976, he was a member of the Department of Electrical and Systems Engineering, Rensselaer Polytechnic Institute, Troy, NY. Since 1976, he has been with the Department of Electrical and Computer Engineering, University of California at San Diego, La Jolla, where he is a Professor and former Department Chairman, working in the area of digital communication theory with special emphasis on spread-spectrum communication systems. He has also been a consultant to both government and industry in the areas of radar and communications.

Dr. Milstein was an Associate Editor for Communication Theory for the IEEE TRANSACTIONS ON COMMUNICATIONS, an Associate Editor for Book Reviews for the IEEE TRANSACTIONS ON INFORMATION THEORY, an Associate Technical Editor for the *IEEE Communications Magazine*, and the Editor-in-Chief of the IEEE JOURNAL ON SELECTED AREAS IN COMMUNICATIONS. He was the Vice President for Technical Affairs in 1990 and 1991 of the IEEE Communications Society, and has been a member of the Board of Governors of both the IEEE Communications Society and the IEEE Information Theory Society. He is a former Chair of the IEEE Fellows Selection Committee, and a former Chair of ComSoc's Strategic Planning Committee. He is a recipient of the 1998 Military Communications Conference Long Term Technical Achievement Award, an Academic Senate 1999 UCSD Distinguished Teaching Award, an IEEE Third Millennium Medal in 2000, the 2000 IEEE Communication Society Armstrong Technical Achievement Award, and the 2002 MILCOM Fred Ellersick Award.

Paul H. Siegel (M'82-SM'90-F'97) received the S.B. degree in mathematics in 1975 and the Ph.D. degree in mathematics in 1979, both from the Massachusetts Institute of Technology (MIT), Cambridge.

He held a Chaim Weizmann Postdoctoral Fellowship at the Courant Institute, New York University. He was with the IBM Research Division in San Jose, CA, from 1980 to 1995. He joined the faculty of the School of Engineering at the University of California, San Diego in July 1995, where he is currently Professor of Electrical and Computer Engineering. He is affiliated with the California Institute of Telecommunications and Information Technology, the Center for Wireless Communications, and the Center for Magnetic Recording Research where he currently serves as Director. His primary research interests lie in the areas of information theory and communications, particularly coding and modulation techniques, with applications to digital data storage and transmission.

Prof. Siegel was a member of the Board of Governors of the IEEE Information Theory Society from 1991 to 1996. He served as co-Guest Editor of the May 1991 Special Issue on Coding for Storage Devices of the IEEE TRANSACTIONS ON INFORMATION THEORY, and served the same Transactions as Associate Editor for Coding Techniques from 1992 to 1995, and as Editor-in-Chief from 2001 to 2004. He was also Co-Guest Editor of the May/September 2001 two-part issue on The Turbo Principle: From Theory to Practice of the IEEE JOURNAL ON SELECTED AREAS IN COMMUNICATIONS. He was co-recipient, with R. Karabed, of the 1992 IEEE Information Theory Society Paper Award and shared the 1993 IEEE Communications Society Leonard G. Abraham Prize Paper Award with B. Marcus and J. K. Wolf. He holds 17 patents in the area of coding and detection, and was named a Master Inventor at IBM Research in 1994. He is also a member of Phi Beta Kappa.